Anoxic-biocathode microbial desalination cell as a new approach for wastewater remediation and clean water production

Simone Perazzoli, José Pedro de Santana Neto and Hugo M. Soares

ABSTRACT

Bioelectrochemical systems are emerging as a promising and friendly alternative to convert the energy stored in wastewater directly into electricity by microorganisms and utilize it *in situ* to drive desalination. To better understand such processes, we propose the development of an anoxic biocathode microbial desalination Cell for the conversion of carbon- and nitrogen-rich wastewaters into bioenergy and to perform salt removal. Our results demonstrate a power output of 0.425 W m^{-3} with desalination, organic matter removal and nitrate conversion efficiencies of 43.69, 99.85 and 92.11% respectively. Microbiological analysis revealed *Proteobacteria* as the dominant phylum in the anode (88.45%) and biocathode (97.13%). While a relatively higher bacterial abundance was developed in the anode chamber, the biocathode showed a greater variety of microorganisms, with a predominance of *Paracoccus* (73.2%), which are related to the denitrification process. These findings are promising and provide new opportunities for the development and application of this technology in the field of wastewater treatment to produce cleaner water and conserve natural resources.

Key words | bioelectrochemical systems, bioenergy, desalination, pollutants removal, water reuse

Simone Perazzoli (corresponding author)
Hugo M. Soares
Department of Chemical and Food Engineering,
Federal University of Santa Catarina,
88034-001 Florianópolis, SC,
Brazil
E-mail: *perazzoli.simone@gmail.com*

José Pedro de Santana Neto
Department of Mechanical Engineering,
Federal University of Santa Catarina,
88034-001 Florianópolis, SC,
Brazil

INTRODUCTION

Due to global warming, population growth, urbanization and increasing consumption of water and energy, the world is ever more focused on the conservation of these, two resources. Although wastewaters are known to have high pollution potential, with the presence of pathogens, hydrocarbons, metals and nutrients, they are a potential source for renewable energy generation due to their high energetic value. In this context emerges the concept of bioelectrochemical technologies (BES). BES applications are attractive as a complement to traditional wastewater treatment technologies, reducing energy requirements as well as recovering resources and synthesizing new products by using wastes as raw material. However, the small amount of energy generated would be sufficient only for low-power applications. Alternatively, it would be an advantage to utilize the electricity to conduct desalination (Al-Mamun *et al.* 2018) or even to synthesize new products. In this context, we emphasize microbial desalination cells (MDCs). These devices enable conversion of the energy stored in wastewater directly into electricity by microorganism activity and utilization of it *in situ* to drive the desalination process, producing clean water (Wang & Ren 2013; Dong *et al.* 2017).

Numerous studies are proving the concept of MDCs using chemicals, e.g. potassium ferricyanide, as electron acceptor (Saba *et al.* 2017). However, due to their toxicity, new alternatives have been developed, such as biocathodes (Kokabian *et al.* 2018a, 2018b; Zuo *et al.* 2018) enabling nutrients removal and recovery and synthesis of valuable bioproducts. Therefore, biocathodes appear as a promising alternative, due to their potential for self-regeneration, scalability and sustainable nature (Al-Mamun *et al.* 2018). In biocathodes, the microorganisms accept the electrons directly from the electrode surface reducing the compounds of interest and, thus, improving the coulombic and desalination efficiencies (Wen *et al.* 2012).

According to the electron acceptor, they are classified into oxic or anoxic (Santoro *et al.* 2017; Al-Mamun *et al.* 2018). In oxic biocathodes, O_2 is the most popular electron acceptor due to its high redox potential (+0.82 V) (Logan *et al.* 2006), having bacterial or microalgae consortia as biocatalysts (Meng *et al.* 2017; Arana & Gude 2018; Zhang *et al.*

doi: 10.2166/wst.2020.134

2019). However, its main disadvantage is associated with dissolved oxygen supply, increasing system operational costs. Due to these limitations, new research has been directed towards the development of anoxic biocathodes. In the absence of O_2, a variety of compounds (e.g. NO_3^-, NO_2^-, SO_4^-, Fe, Mn, selenate, arsenate, urinate, fumarate and CO_2) could be employed as the final electron acceptor, in which nitrate presents redox potential (+0.74 V) comparable to O_2.

The use of denitrifying bacteria to reduce nitrate in BES dates back to 1966 (Lewis 1966). However, this concept has been experimentally validated only in recent years (Clauwaert *et al.* 2007; Srinivasan *et al.* 2016; Wang *et al.* 2016). Recently, Kokabian *et al.* (2018b) developed an MDC using a consortium of anammox bacteria as biocatalysts achieving a maximum current density of 0.814 A m^{-3} (0.092 W m^{-3}), and ammonium nitrogen conversion higher than 90% with nitrate accumulation and desalination efficiency of 25.5%.

Because of the above-mentioned points, the development of biocathode MDCs is emerging as a promising alternative; however, this process needs to be better understood and exploited, particularly when it comes to the establishment of anoxic biocathodes for nitrate reduction via the autotrophic denitrification process (Cecconet *et al.* 2019). In this study, we established a novel MDC operating with an anoxic biocathode to remediate carbon- and nitrogen-rich wastewaters, generating bioelectricity with additional salt removal, aiming for the reuse and conservation of water resources. Investigations in this field are strongly helpful, bringing new possibilities to couple such systems with those already existing, reducing energy requirements as well as recovering resources and synthesizing new products by using wastes as raw material.

MATERIALS AND METHODS

Reactor design

The MDC operating with an anoxic biocathode (Anox-Bio-MDC) reactor was constructed of polyvinyl chloride, consisting of three chambers with the following net liquid volume: anode (0.8 L), cathode (0.8 L) and desalination (0.31 L). The desalination chamber was separated from anode and cathode by a compartmental anion exchange membrane (AEM; AMI-7001S) and cation exchange membrane (CEM; CMI-7000S), spaced 5 cm from each other. Commercial granular activated carbon (GAC, ~670 μm) produced from coconut shell (Smart Carbon, Brazil) packed in a stainless-steel metallic fabric (mesh 200 – Telas Rocha Ltd, Brazil) cartridge (length: 15.0 cm, diameter: 2.0 cm, GAC mass: 15 g) was used to build electrodes. Six packaged cartridges were added to each chamber. This strategy was chosen aiming to increase the electrode contact area available for microorganisms and also to avoid loss of GAC mass during system operation. To collect electrons, we used stainless-steel fabric in the cartridges and connected it to an external cable collector. The bioreactor configuration is shown in Figure 1.

Enriched culture, medium and system operation

The anode was inoculated with a mix of anaerobic sludge from a municipal wastewater treatment plant and denitrifying sludge from a shrimp wastewater treatment pilot system (SWTP) (1:1, v/v, volatile suspended solids 1.70 ± 0.2 g L^{-1}), while the cathode was inoculated only with denitrifying sludge from the SWTP with the same biomass concentration. This inoculum source was selected as the bacteria were already adapted to salinity >15‰. Nutrient medium was based on Lovley & Phillips (1988), containing (per L): 2.5 g $NaHCO_3$, 0.1 g $CaCl_2.2H_2O$, 0.1 g KCl, 0.6 g $NaH_2PO_4.H_2O$, 1.87 g $Na_2HPO_4.12H_2O$, 0.1 g NaCl, 0.1 g $MgCl_2.6H_2O$, 0.1 g $MgSO_4.7H_2O$, 0.005 g $MnCl_2.4H_2O$ and 0.05 g of yeast extract. The same medium composition was adopted for anode and cathode, at pH 7.0; meanwhile, acetate (2.0 g L^{-1}) was the electron donor and nitrate (0.05 g L^{-1}) was the electron acceptor.

To promote the electroactive biofilm growth and acclimatization (Babauta *et al.* 2012), the system was initially operated under open-circuit voltage (OCV), enabling the development of a stable biofilm on the electrode surface through natural redox processes. After voltage stabilization, external resistors (560, 100 and 22 Ω) were connected between the anode and cathode, closing the circuit (CCV) and improving the electron transfer through the circuit. In both operational stages, anode and cathode chambers were operated under fed-batch mode with cycles of 12 hours and a feed rate of 0.6 L d^{-1} (hydraulic retention time, HRT of 1.33 days), while the desalination chamber was operated under fed-batch mode with cycles of 8 days and a feed rate of ~0.039 L d^{-1} (HRT of 8 days). It is worth mentioning that HRT was computed by the relation V/Q, where V represents the volume of the system (L) and Q is the influent flow-rate (L d^{-1}).

Kinetic assays

Kinetic assays were performed to achieve substrate conversion rates. Here acetate is expressed in terms of COD (chemical oxygen demand), nitrate in terms of NO_3^--N, and

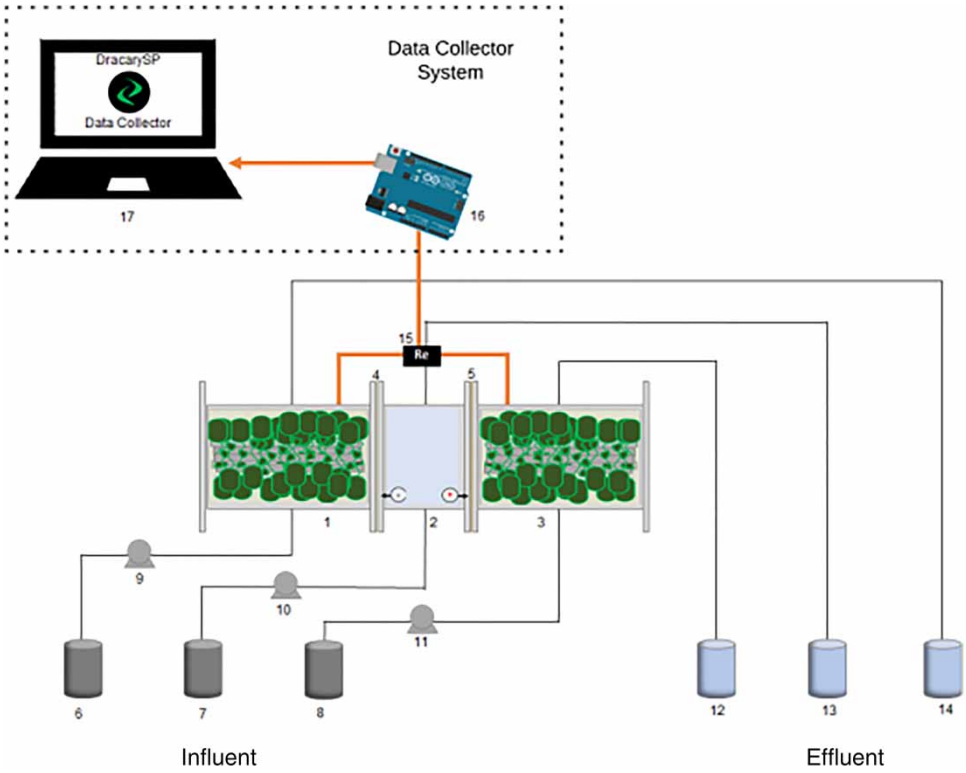

Figure 1 | Schematic representation of the ANOX-BIO-MDC system: 1 – anodic chamber; 2 – desalination chamber; 3 – cathodic chamber; 4 – AEM; 5 – CEM; 6, 7 and 8 – influent (inputs) of 1, 2 and 3; 9,10 and 11 – feed pumps; 12, 13 and 14 – effluent (outputs) of 1, 2 and 3; 15 – external circuit; 16 and 17 – data acquisition system composed of a microcontroller Arduino Uno (16) connected to a laptop (17).

saline solution in terms of electrical conductivity (EC). For anode and cathode kinetics, the concentration of the saline solution was fixed at 10 g NaCl L^{-1}. When the system achieved operational stabilization at a 22 Ω resistor (condition that gave us the best carbon and nitrogen conversion rates ('Organic matter conversion' and 'Nitrogen conversion' sections)), the influence of salt concentration on desalination performance was investigated. The following saline solutions were evaluated (g NaCl L^{-1}): A (10.00), B (20.00) and C (35.0). Additional tests were performed by replacing the synthetic solution with seawater (D).

Analysis and data acquisition

COD and nitrogen species (NH_4^+-N, NO_2^--N and NO_3^--N) were determined through the colorimetric method (APHA 2012). For voltage and EC measurements, a device based on an Arduino microcontroller was constructed. For data acquisition and monitoring in real-time (sampling interval of one second), custom software was developed using Python (available at https://github.com/simoneperazzoli/dracarys-project). For EC measurements, an analog EC probe designed for Arduino microcontrollers (Analog EC Meter, DFRobot©) was used. Polarization curve tests, which are used to characterize current as a function of voltage, were carried out when the system reached stability at OCV condition, according to Watson & Logan (2011) methodology. Each resistance was tested for two consecutive operational cycles (24 hours) to ensure a stable voltage response. The following resistors were applied (Ω): 10,000, 5,600, 1,000, 560, 220, 100, 47, 22 and 4.6.

To investigate the biofilm formation, scanning electron microscopy (SEM) analysis was performed. Anode and biocathode samples were prepared according to Perazzoli *et al.* (2018). Samples were examined under a JEOL microscope (SEM JSM-6390LV), operated at 15 kV (LCME/UFSC, Brazil). The microbiological profile of the biofilm developed on the surface of the electrodes was analyzed through 16S rDNA sequencing analysis, according to Christoff *et al.* (2017). Detailed information about the sample preparation and procedures are presented in the Supplementary Information.

Data post-processing

All data obtained were post-processed using Python software with NumPy and SciPy libraries. In the case of

voltage data (obtained in digital form), the Savitzky–Golay smooth filter (Savitzky & Golay 1964) was applied, to minimize random noise effects.

Coulombic efficiency (CE), current density and power density were normalized by the anode chamber volume and computed according to Logan (2008). Internal resistance was estimated through the graphical analysis of the polarization curve in the region of constant voltage drop as a function of the current produced (Watson & Logan 2011). For kinetic assays, the respective rates (in terms of mass per volume per time) were determined graphically, by finding the slope of the concentration curve against time. Rates were computed according to Hui *et al.* (in press). The interval between higher substrate consumption and product generation (observed in the initial 3 hours of kinetics) or salt removal (observed in the first 2 days of measuring) was considered. Efficiencies of COD removal, nitrate conversion and desalination were computed as:

$$EF_C(\%) = \left(\frac{C_t - C_{to}}{C_{to}}\right) * 100$$

where C_t and C_{to} refer to the final and initial concentrations of a given compound during an operating cycle.

RESULTS AND DISCUSSION

Acclimatization at open-circuit voltage

The first stage of Anox-Bio-MDC reactor operation was under OCV condition, where current is null and the voltage produced is the maximum. As presented in Figure 2(a), initially, there is an adaptation or lag phase that goes until the third day. The higher bacterial activity (maximum voltage rate of 91 mV d^{-1}) was observed between the fourth and eighth days of inoculation. After this period, the system reached the steady-state phase, and its maximum potential was achieved in the twenty-sixth day (563 mV). After that, the voltage remained stable at ~544.5 mV. These values are higher than previously reported for bio-MDCs. By incorporating *Nanochloropsis salina* into the cathode of an MDC, Girme (2014) observed a maximum OCV potential of 98.2 mV. Here, our strategy proved to be efficient, allowing the development of a stable microbial community (Babauta *et al.* 2012).

Energy potential

The polarization curve is presented in Figure 2(b). The maximum power density observed was 0.425 Wm^{-3}, which is 2.8 times higher than reported for an MDC operating with *Chlorella vulgaris* sp. biocathode (Kokabian & Gude 2013) and 4.6 times higher than reported for an MDC operating with anammox biocathode (Kokabian *et al.* 2018b). Internal resistance (Ri) was 115.7 Ω, which is close to that reported by Meng *et al.* (2017) (94.2 Ω) and 26 times lower than observed by Kokabian *et al.* (2018b) (3,101 Ω), indicating good performance of our system.

According to Ohm's Law, the external resistance (Re) controls the electron flow from anode to cathode, affecting directly the potential and the current passing through the system. As reported in Figure 3, as the Re load decreases, there is a significant drop in voltage values, contrary to

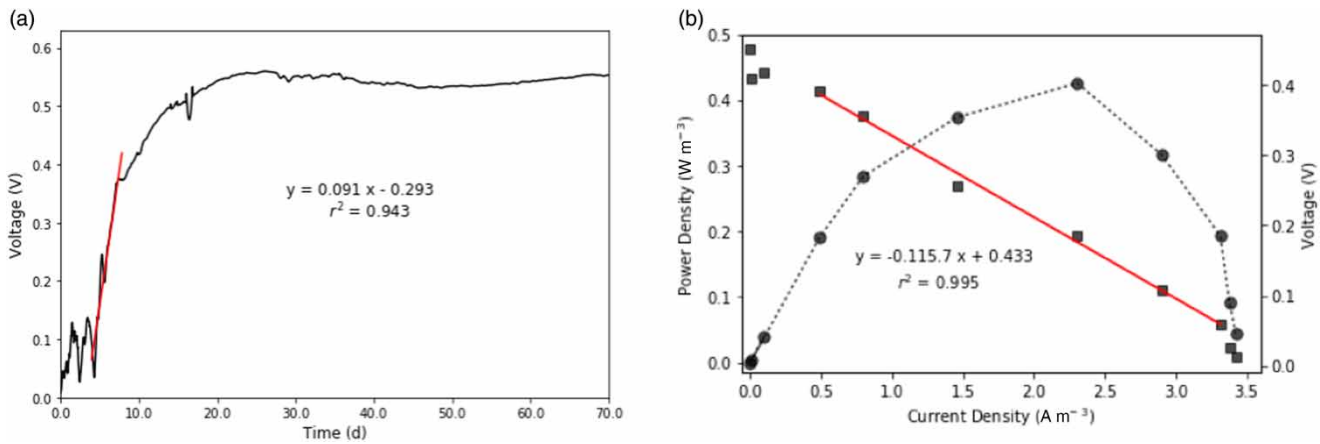

Figure 2 | Voltage profile during the Anox-Bio-MDC startup (a) and polarization and power curve obtained during the Anox-Bio-MDC operation, where squares represent voltage and circles represent the power density behavior (b).

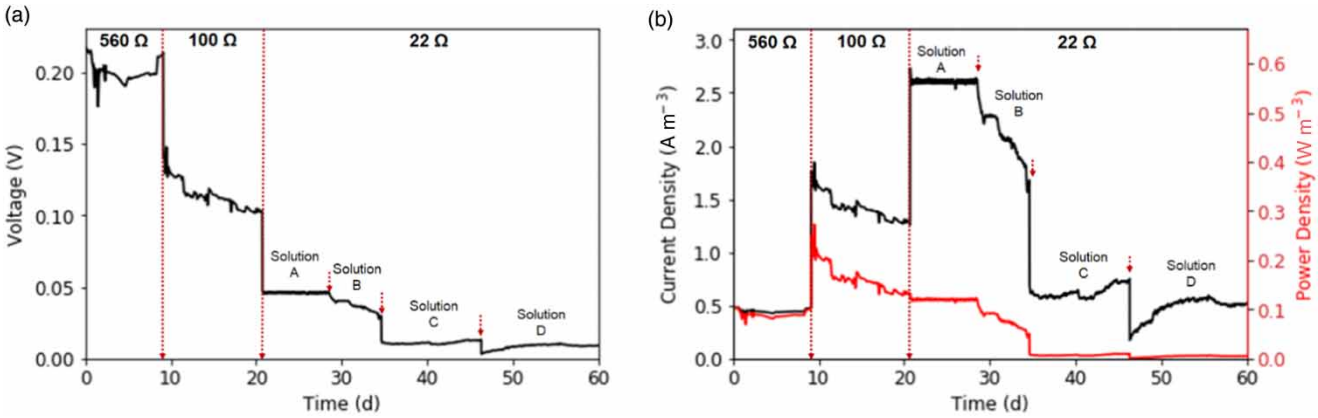

Figure 3 | Voltage (a), current and power densities (b) profiles obtained during CCV operation. In part (b), black line refers to current density and grey line refer to power density.

current density behavior, which gradually increases up to 2.61 A m^{-3} (Table 1). These results show that the ohmic losses were dominant in this operational stage (Lefebvre *et al.* 2008). At 22 Ω resistance, there were significant variations in the voltage, current and power density values (Figure 3(a) and 3(b)). This is due to the conductivity of the saline solution. Thus, as the conductivity in the desalination chamber increases, the higher is the ion migration between the chambers and, therefore, there is a higher internal current consumption to perform the desalination process. Also, a significant drop in power density was observed. This is because the system was operated with Re lower than Ri, as previously reported by Logan (2008). Electric coefficients obtained during reactor operation are presented in Table S1 (Supplementary Information).

Organic matter conversion

According to the kinetic assays, the highest acetate consumption rate was observed in the first hours of the cycle (Figure 4(a)). From these assays, the maximum COD conversion rates ($-r_{COD}$) were obtained. As presented in Figure 4(b), for OCV condition, the $-r_{COD}$ was 212.4 mg L^{-1} h^{-1}, while it was 37.95% higher (293.01 mg L^{-1} h^{-1}) for 22 Ω condition. COD removal efficiencies were improved from 75.7% to 99.85%. The pollutant removal was improved with the load resistor decrease. This strategy allows the reduction of the overpotentials, increasing, therefore, the electron transfer rate through the circuit (Katuri *et al.* 2011). These values are in agreement with Zhang *et al.* (2019) and higher than those previously reported for biocathode MDCs (see Table 2). COD removal efficiencies of between 40 and 60% were achieved by Kokabian *et al.* (2018a, 2018b). Meng *et al.* (2014, 2017) evaluated two MDC configurations to treat dewatered sludge, with organic matter removal efficiencies between 14.7 and 25.7%.

Coulombic efficiency was improved from 5.01 to 28.32% by reducing Re load. Besides the improvement, 71.68% of oxidized organic matter was not converted into electricity, indicating the COD removal by non-electrogenic mechanisms (Cecconet *et al.* 2018; Mologni *et al.* 2018). According to Vilajeliu-Pons *et al.* (2016), an alternative for improving the CE could be the application of a variable resistance control to enhance the electron transfer, as intermittent electric connection allows higher current production since both capacitive and faradaic currents are harvested.

Table 1 | Electric coefficients obtained during Anox-Bio-MDC reactor operation

				22 Ω			
	OCV	560 Ω	100 Ω	A	B	C	D
Voltage (V)	0.544	0.201	0.114	0.049	0.039	0.011	0.008
Current density (A m^{-3})	n.a.	0.450	1.423	2.611	2.204	0.623	0.474
Power density (W m^{-3})	n.a.	0.090	0.162	0.110	0.581	0.007	0.004
CE (%)	n.a.	5.00	15.46	28.35	23.94	6.77	5.15

Note: Standard deviation <0.001 for all cases.

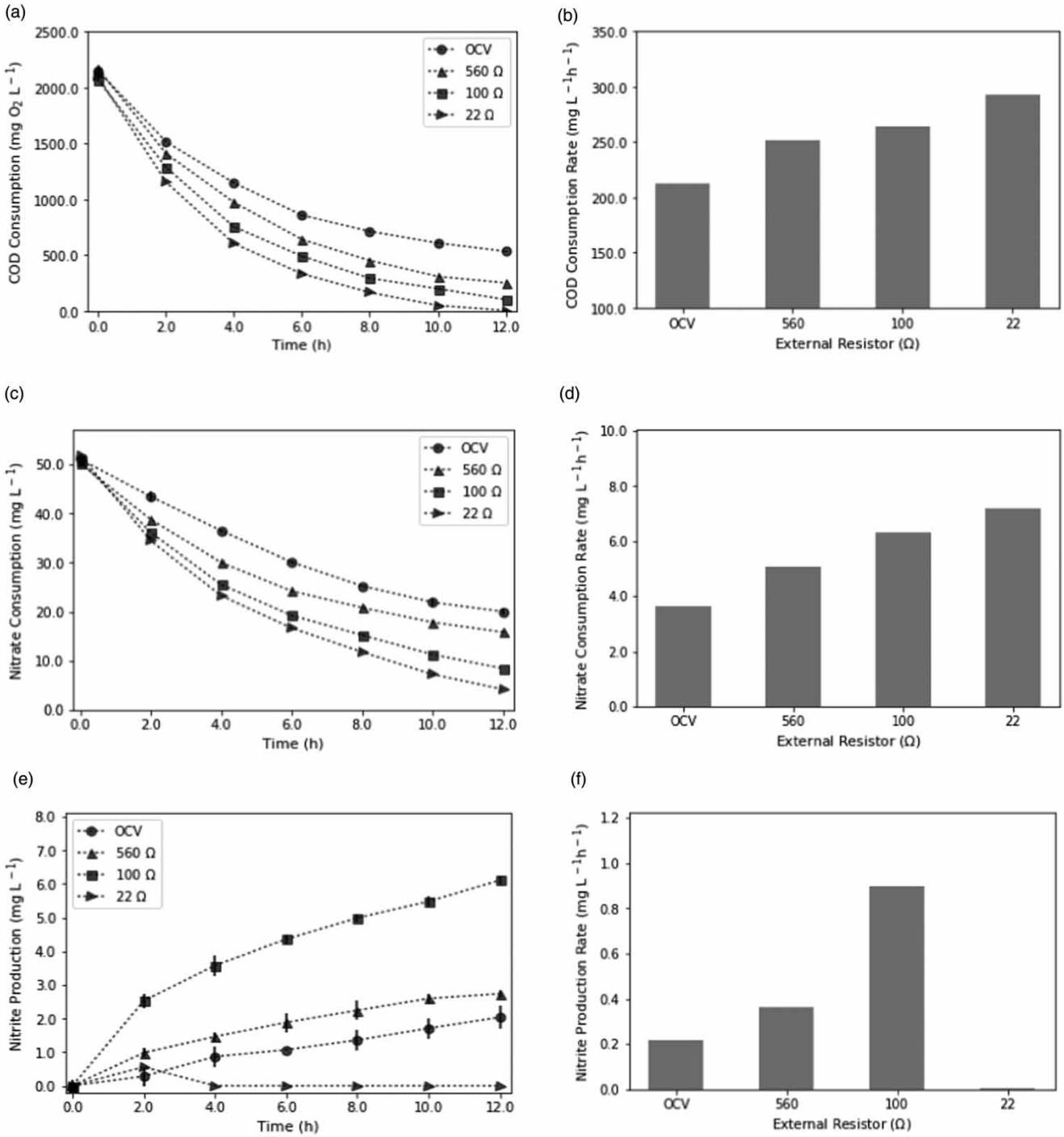

Figure 4 | Substrate conversion during OCV and CCV operational conditions: COD kinetic assays (a) and conversion rate values (b); nitrate kinetic assays (c) and conversion rate values (d); kinetic assays for nitrite formation (e) and accumulation rate values (f).

Nitrogen conversion

Electroautotrophic denitrification processes have gained widespread attention in recent years (Chen *et al.* 2016; Xu *et al.* 2017; Cecconet *et al.* 2019). In the present study, during the startup and acclimatization, there was observed a gradual increase in denitrification rates, indicating the establishment of electroactive biofilm. From the kinetic

Table 2 | Comparison between studies reported in the literature using MDC with biocathode

	Inoculum source				Electric parameters			Desalination				
Configuration	**Anode**	**Cathode**	**Electron donor**	**Electron aceptor**	**Re (kΩ)**	**V (mV)**	**I (mA)**	**EF_d (%)**	**HRT (days)**	**EF_{COD} (%)**	**EF_N (%)**	**Reference**
MDC	Sludge dehydrated	Surface soil bacterial consortium	Sludge dehydrated	O_2	1.0	800.0	0.80	40.3	3.0	25.7	n.a	Meng *et al.* (2014)
MCDC	Sludge dehydrated	Consortium previously enriched in MDC	Sludge dehydrated	O_2	1.0	864.0	0.86	12.9	1.0	14.7	n.a	Meng *et al.* (2017)
PMDC	Consortium enriched from aerobic sludge	*Chlorella vulgaris*	Glucose	O_2	10.0	236.0	0.023	40.1	>25.0	56.6	n.a	Kokabian & Gude (2013)
PMDC	Consortium enriched from aerobic sludge	*Chlorella vulgaris*	Glucose	O_2	1.0	167.0	0.167	26.2	>6.0	60.0	n.a	Kokabian *et al.* (2018a)
PMDC	Aerobic sludge	Consortium enriched in an algal cathode MFC	Glucose	HCO_3	1.0	206.0 to 256.0	0.206 to 0.256	33.4 to 47.1	~2.8	n.a	n.a	Arana Gude (2018)
Anammox-MDC	Anaerobic sludge	Anammox consortium	Glucose	NH_4^+/ NO_2^-	1.0	89.6	0.09	25.5	>10.0	40.0	N-H_4^+: >90.0	Kokabian *et al.* (2018b)
MDC	Anaerobic sludge	Aerobic sludge	Domestic wastewater	O_2	1.0	510.0 to 640.0	0.51 to 0.64	97.4	>45.0	94.6	N_{total}: 99.8	Zhang *et al.* (2019)
Anox-Bio-MDC	**Denitrifying/ anaerobic consortium**	**Denitrifying consortium**	**Acetate**	**NO_3^-**	**0.022**	**49.0 to 8.0**	**2.23 to 0.36**	**24.42 to 43.69**	**8.0**	**99.85**	**N-NO_3^-: 92.11**	This study

MCDC: microbial capacitive desalination cell, PMDC: photosynthetic microbial desalination cell, Re: external resistance, V: cell voltage, I: current, EF_d: desalination efficiency, HRT: hydraulic retention time, EF_{COD}: COD removal efficiency; EF_N: nitrogen conversion efficiency; N_{total}: total nitrogen, n.a.: not available.

assays, the maximum nitrate conversion rates (r_{NO_3}) were obtained (Figure 4(c)). The r_{NO_3} for OCV condition (Figure 4(d)) was 3.65 mg L^{-1} h^{-1}, while the same for 22 Ω condition was 96.44% higher (7.18 mg L^{-1} h^{-1}). NO_3^--N conversion efficiencies were improved from 60.84% to 92.11%, which is 1.31 times higher than observed by Kizilet *et al.* (2015) in a biocathode MFC.

Production and accumulation of nitrite (Figure 4(e)) was also observed. In the OCV conditions, an amount of 2.04 mg L^{-1} ($r_{NO_2} = 0.217$ mg L^{-1} h^{-1}) accumulated at the end of an operational cycle. For CCV conditions, the nitrite accumulation reached 2.74 mg L^{-1} ($r_{NO_2} = 0.365$ mg L^{-1} h^{-1}) for 560 Ω and 6.11 mg L^{-1} ($r_{NO_2} = 0.895$ mg L^{-1} h^{-1}) for 100 Ω, respectively (Figure 4(f)). These results indicate the denitrification process occurred incompletely (Desloover *et al.* 2011; Srinivasan *et al.* 2016). However, at 22 Ω resistance, nitrite accumulation was not observed. According to Clauwaert *et al.* (2007), high resistor load contributes to the accumulation of intermediate compounds in the denitrification process, such as nitrite and nitrous oxide. Thus, an alternative to solve it is to operate the system with lower resistor load, as reported here. It should be mentioned that ammoniacal nitrogen was not detected.

Desalination assay kinetics

In MDCs, the desalination process occurs by two main phenomena: osmotic pressure and ionic concentration difference between compartments. Here, the EC for anolyte and catholyte was 8.51 ± 0.01 and 6.49 ± 0.08 mS cm^{-1}, while the saline solution had an initial EC of 16.58 ± 0.11, 38.84 ± 0.12, 61.35 ± 0.32 and 61.89 ± 0.22 mS cm^{-1} for solutions A, B, C and D, which are higher, compared to the anolyte and catholyte at the beginning of the experiment. This difference could lead to the occurrence of natural osmosis. Thus, the liquid of the lowest conductivity solution migrates to the solution with higher conductivity until the balance between the solutions is established.

The second factor is related to the ion migration between cell compartments. As biological degradation of organic compounds in the anode results in the release of protons and electrons, the anionic species migrate from the desalination chamber to the anode through the AEM. Similarly, the cationic species migrate from the desalination chamber to the biocathode through the CEM. Therefore, the catalytic activity of bacteria, substrate utilization and formation of metabolites play a vital role in forming an electrochemical gradient that will establish the rate of the desalination process (Ashwaniy & Perumalsamy 2017). To assess it, desalination kinetic assays were conducted. As presented in Figure 5, by increasing EC from solution A to D, the desalination rate ($-r_d$) was increased 6.78 times (from 0.95 to 6.43 mS cm^{-1} d^{-1}).

A similar trend was observed for desalination efficiencies and these values agree with those previously reported for biocathode MDCs, as presented in Table 2. Desalination efficiency was improved from 24.42% to 39.71% for solution A to C, respectively. When NaCl solution was replaced by seawater, an increase of 10.02% in desalination efficiency (43.69%) was observed. These results are promising; however, improvements are still needed, especially concerning the increase of the desalination efficiency and reduction of the HRT of the desalination chamber. According to Gude *et al.* (2013), desalination performance in MDCs could be improved by inserting multiple pairs of ion-exchange membranes between the anode and cathode chambers. This strategy improves the charge transfer efficiency and allows the saline water to flow through a series of MDCs leading to more salt removal. In addition, increasing the number of cell pairs reduces the voltage required in each cell, allowing an energy gain.

Moreover, with the use of thin ion exchange membranes and desalination chambers, the internal resistance is reduced and more efficient separation of ions and water desalination can be achieved (Kim & Logan 2011). Kinetic coefficients are presented in Table S1. It is worth mentioning that, during OCV operation, no changes were observed in the conductivity of the desalination chamber solution. This result agrees with that previously reported by Cao *et al.* (2009) and is because under these conditions, there is no current passing through the circuit and, therefore, the ion migration is minimal.

Microbial community morphology

In MDCs, the biofilm developed on the anodic electrode acts as a catalyst, aiding the bacterial respiration, which in turn produces more current (Baranitharan *et al.* 2015). These bacteria transfer extracellularly the electrons obtained in the respiration process towards an exogenous electron acceptor. Thus, the highest power densities are produced by inoculating the anode with a rich and diverse source of bacteria, such as sludge, soil or sediments (Logan 2009). On the other hand, the biofilm developed in the biocathode accepts directly the electrons from the electrode surface, thus reducing compounds (Lovley & Nevin 2011). However, in contrast to exoelectrogens, there are few

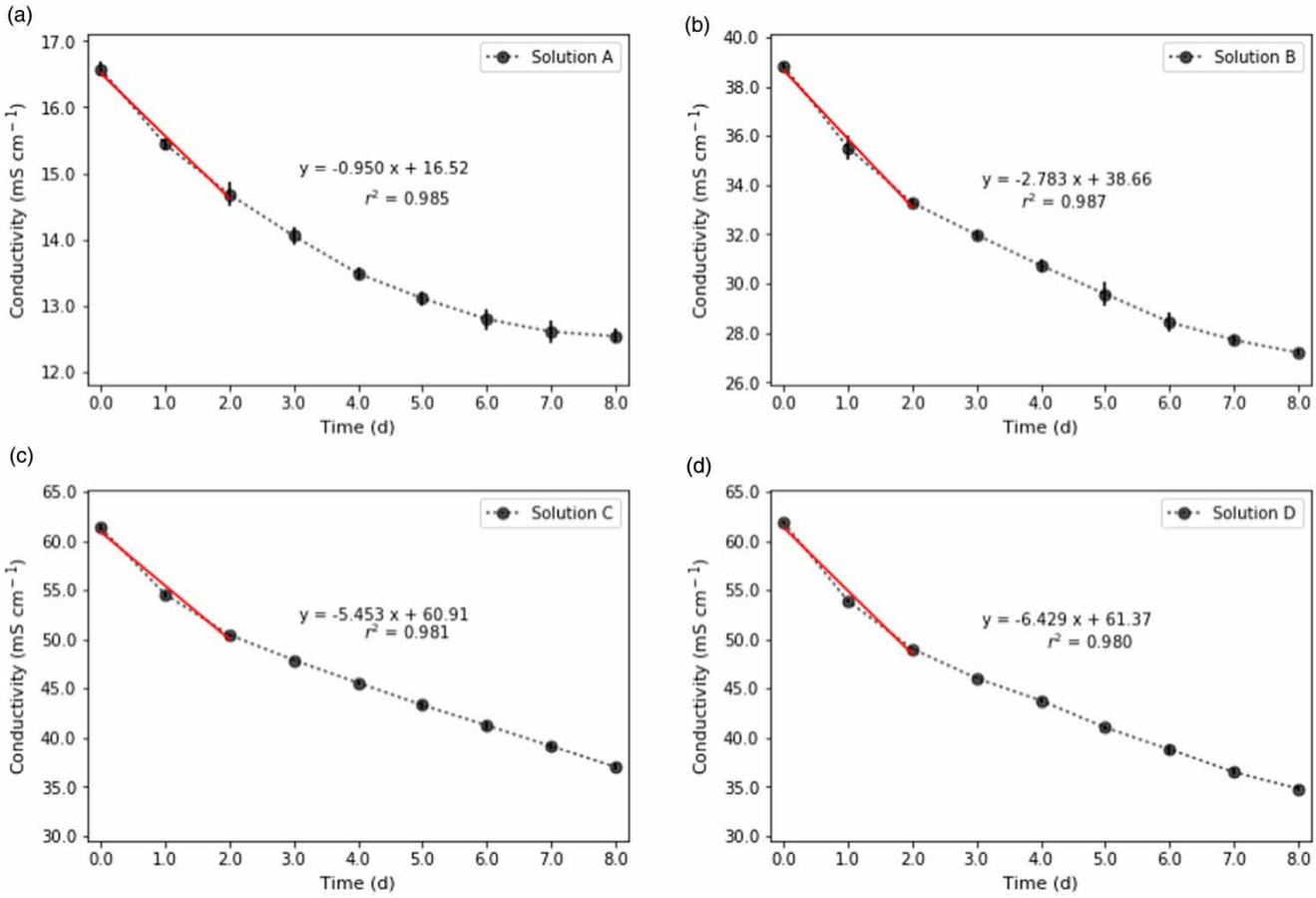

Figure 5 | Desalination kinetics for saline solutions A, B, C and D, respectively.

studies related to electrotrophic characterization (Vilajeliu-Pons *et al.* 2016).

According to literature, the microbial community composition of biofilm is affected by the inoculum source, type of microorganisms (Gram-positive or Gram-negative), nature of microbial culture (pure or mixed) and pre-enrichment and startup strategies (Mologni *et al.* 2014; Saratale *et al.* 2017). Thus, to investigate the morphology of bacterial biofilm developed on the electrode surface, SEM was conducted.

In Figure 6, we can observe the development and enrichment of exoelectrogens (Figure 6(a) and 6(b)) and electrotrophs (Figure 6(c) and 6(d)) with biofilm formation on granular activated carbon electrodes. Electron micrographs show unique biofilm structures and cell shapes. The anode was covered with short-rod and coccoid bacteria, which are similar in cell shape and arrangement to exoelectrogenic bacteria (Bond & Lovley 2003). On the other hand, the nitrate-fed biocathode presented a lower diversity, with a predominance of coccoid-shaped bacteria.

Microbial community abundance

Anodic bacterial diversity and abundance

A relatively higher bacterial abundance was developed in the anode chamber than in the anoxic biocathode chamber. The dominant phyla were *Proteobacteria* (88.45%), where *α-Proteobacteria* (53.24%), *β-Proteobacteria* (15.01%), *δ-Proteobacteria* (8.86%), *γ-Proteobacteria* (7.6%) and *ε-Proteobacteria* (3.75%) were the classes. Other phyla presented in minor proportions were *Thermotogae* (2.87%), *Bacteroidetes* (2.74%) *Euryarcheota* (2.41%), *Actinobacteria* (1.75%) and *Firmicutes* (1.72%) (Figure S2(a)). These results are in agreement with the literature, as there are several reports on BES containing diverse microbial communities, in which electrical current generation has been shown by *Proteobacteria*, *Firmicutes* and *Acidobacteria* phyla (Li *et al.* 2014; Zhang *et al.* 2015, 2016).

Herein, the main genera identified in the anode chamber are presented in Figure 7(a). *Paracoccus* showed

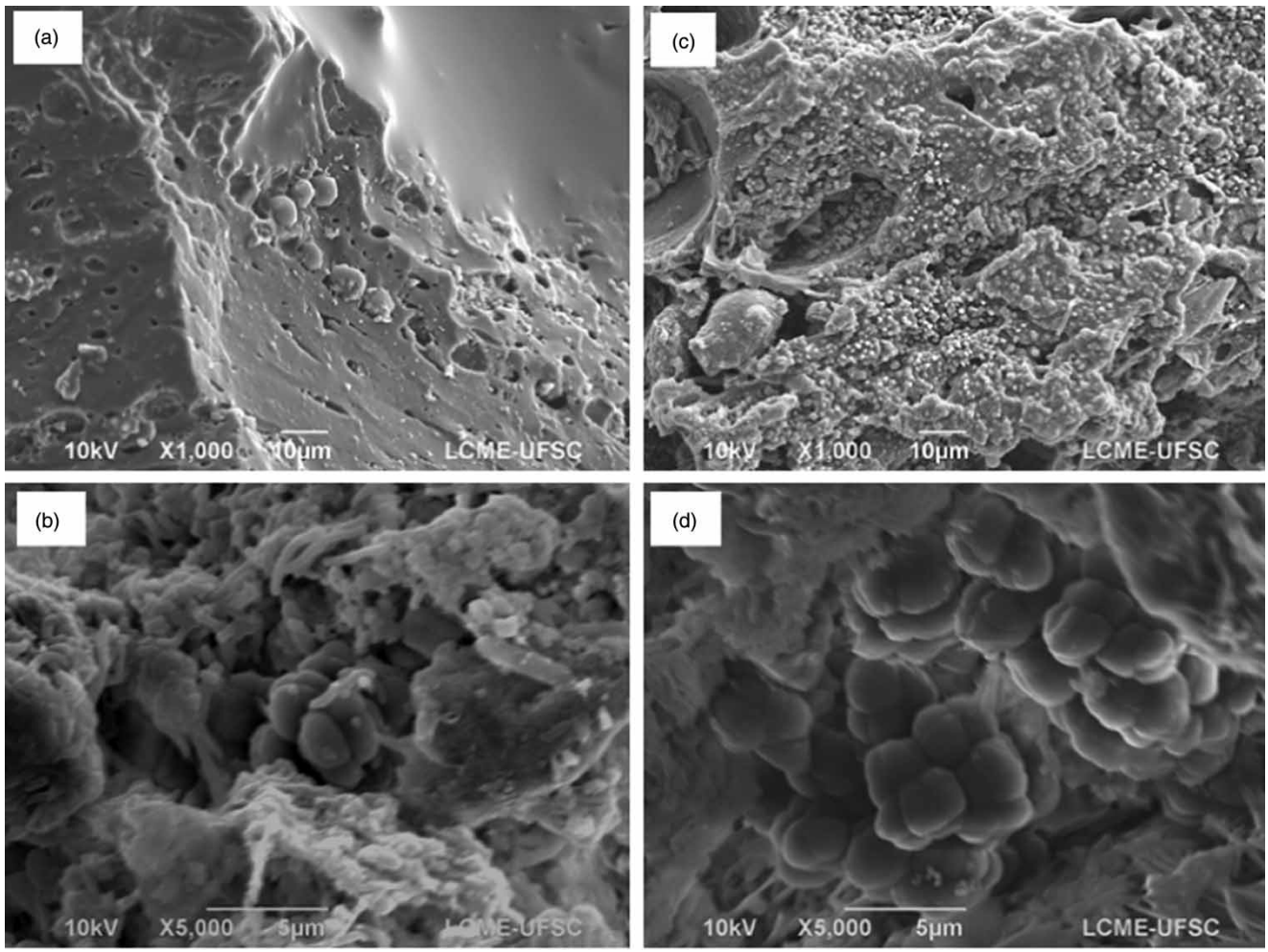

Figure 6 | SEM image of the anodic electrode surface (a) following growth of exoelectrogenic bacteria (b), and cathodic electrode surface (c) following growth of electrotrophic bacteria (d).

the highest number of sequences (2,531), followed by *Stappia* (1,414), *Desulfomicrobium* (1,268), *Rhizobium* (1,124), *Alcaligenes* (997) and *Aquamicrobium* (963). *Paracoccus* and *Stapia* genera belong to the *Rhodobacterales* order. *Paracoccus* spp. include common types of denitrifier species (e.g. *P. pantotrophus*, *P. denitrificans*) which can grow under aerobic or anaerobic conditions. However, these bacteria have also the ability to oxidize carbon and sulfur compounds and produce bioelectricity, as previously reported (Jothinathan & Wilson 2018).

Desulfomicrobium is a strictly anaerobic genus of sulfate-reducing bacteria, which has been reported to consume organic substances in bioelectrochemical systems (Cao *et al.* 2018; Gacitúa *et al.* 2018). The *Rhizobiales* order was also identified, having *Rhizobium* spp. as the main representative (7.8%). These bacteria were previously identified in the anode biofilm enriched from rice paddy soil (Ishii *et al.* 2008) and also in a microbial fuel cell for Congo red decolorization (Hou *et al.* 2011), suggesting a possible involvement of these microorganisms in the current generation.

Alcaligenes composed 6.9% of the microbial community diversity. These are facultative anaerobic bacteria that are able to produce hydrogen, denitrify and also produce electrical current. In the latter case, the electron transfer is associated with the presence of plastocyanin, a mediator excreted by these species (Young *et al.* 2011). *Aquamicrobium* spp. was identified in proportions similar to that reported for BES treating recalcitrant organics with simultaneous electricity generation (Cheng *et al.* 2015). Several other microorganisms related to the current production were identified in a minor proportion, such as *Brevundimonas* (3.6%), *Thauera* (3.4%), *Pseudochrobactrum* (3.3%), *Devosia* (3.3%), *Delftia* (3.2%), *Mesotoga* (3.0%), *Methanosarcina* (2.5%), *Halothiobacillus* (2.4%), *Macellibacteroides* (2.0%), *Pseudomonas* (1.7%), *Alcanivorax* (1.6%) and *Achromobacter* (1.5%) (Wenzel *et al.* 2017; Zhang *et al.*

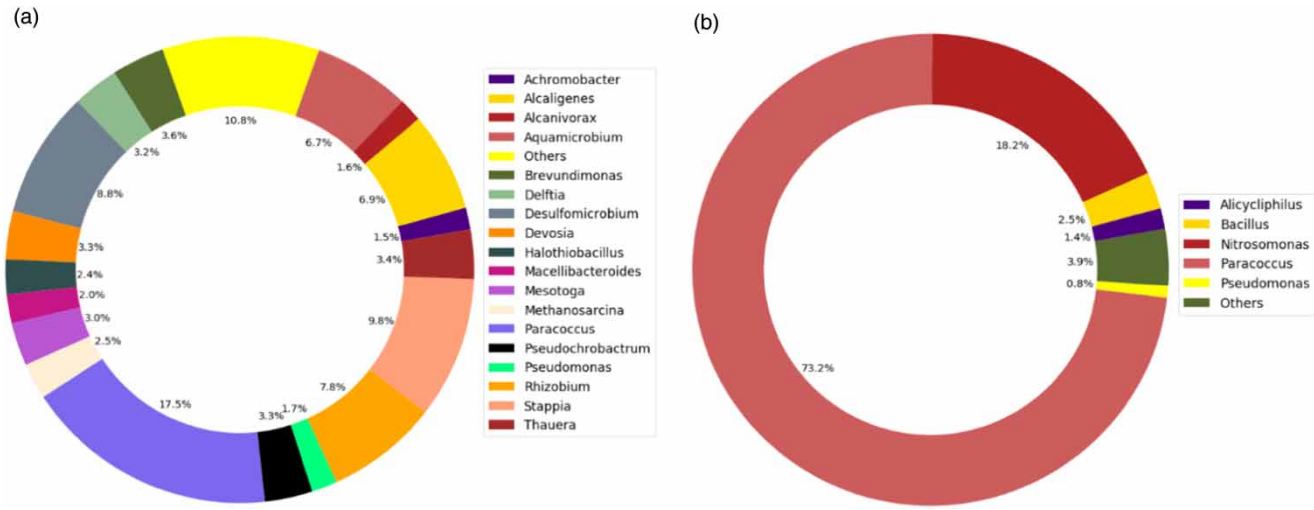

Figure 7 | Microbial community genus developed in the anodic (a) and anoxic biocathode (b) chambers, respectively (sequencing number <100).

2017). Studies have shown that current generation by *Delfia* species is associated with the excretion of secondary metabolites, as occurs with *Pseudomonas* spp. through phenazines excretion (Qiao *et al.* 2017).

Halothiobacillus neapolitanus presence suggests potential for CO_2 fixation (Menon *et al.* 2008), while the presence of bacteria belonging to the genera *Thauera*, *Pseudochrobactrum*, *Alcanivorax* and *Achromobacter* suggests the potential for remediation of environments contaminated by metals, phenols, hydrocarbons and quinones with concomitant bioelectricity generation and desalination (Wang *et al.* 2017). On the other hand, the presence of *Macellibacteroides*, *Mesotoga* and *Methanosarcina* genera indicates the presence of fermentative and methanogenic bacteria competing with the exoelectrogenic ones for the substrate, because a large fraction of the added substrate (71.68%) was not converted into electricity (Mologni *et al.* 2018). It is worth mentioning that *Geobacter* and *Shewanella* species, model microbes for exoelectrogenic studies (Rotaru *et al.* 2014), were not observed in this study, probably due to the inoculum nature.

Anoxic biocathode bacterial diversity and abundance

Denitrifier identification is essential to reveal the microbiological mechanisms and to optimize the denitrification process (Xing *et al.* 2018). *Proteobacteria* phylum was dominant in the anoxic biocathode (97.13%), where *α-Proteobacteria* (75.16%) and *β-Proteobacteria* (20.89%) were the dominant classes. *Firmicutes* phylum was also identified (see Figure S2(b)). These results confirm that *α-Proteobacteria* classes can improve current production and nitrate removal performance (Qiao *et al.* 2017; Sun *et al.* 2017). The dominant species were those belonging to the *Paracoccus* genus with 30,542 sequences (Figure 7(b)).

Unlike the anode, the anoxic biocathode showed less diversity, and *Paracoccus pantotrophus* was the dominant species (70.98%), confirming the predominance of coccoid bacteria observed in SEM micrographs (Figure 6(d)). Cheng *et al.* (2017) reported the ability of *Paracoccus* species to receive electrons from the surface of the cathodic electrode in MFCs conducting electroautotrophic denitrification, as occurs with *Alicycliphilus* species (Tang *et al.* 2017), identified in less proportion (1.4%). *Paracoccus pantotrophus* is among the dominant mixotrophs, which can grow autotrophically, heterotrophically or mixotrophically, both under aerobic or anaerobic conditions, which justifies its presence in the anode. When these microorganisms grow autotrophically (as in the biocathode), the respiratory metabolism can use nitrate, nitrite or nitrous oxide as the final electron acceptor enabling the conversion of most of the oxidation products into nitrogen gas (Liu *et al.* 2017).

A considerable amount of *Nitrosomonas* spp. was identified, including *N. europaea* (16.30%) and *N. eutropha* (2.30%). These species can grow in aerobic or even anaerobic ammonia oxidation. However, under anoxic conditions, these bacteria can also grow via denitrification. In this case, nitrite is used as the final electron acceptor (Schmidt *et al.* 2004). This is explained by the prevalence of *cytL* and *cytS* genes, suggesting their involvement in the oxidation/reduction and electron transfer reactions for energy generation (Caranto *et al.* 2016). *Bacillus* species were identified in the proportion of 2.6% (1,044 sequences). Studies have shown that these microorganisms can grow under anoxic

conditions, using nitrate or nitrite as a final electron acceptor, in addition to producing electric current (Yoganathan & Ganesh 2015). Other genera related to the denitrifying activity (3.9%) were identified in smaller proportions (>100 sequences each). The main microorganism species identified are presented in Figure S3.

CONCLUSIONS

This study demonstrates the potential of MDCs operating with anoxic biocathode for electroautotrophic nitrate reduction as an eco-friendly technology to remediate carbon- and nitrogen-rich wastewaters, enabling energy recovery and *in situ* desalination. Our results show an additional power generation of 0.425 W m^{-3} with suitable salt removal efficiencies. Furthermore, carbon and nitrate conversions higher than 90% were observed.

Despite the challenges related to the implementation of such technologies, this study brings new opportunities for the development and application of bioelectrochemical reactors for wastewater treatment and cleaner water production.

ACKNOWLEDGEMENTS

Authors thank financial support from CAPES and CNPQ.

SUPPLEMENTARY MATERIAL

The Supplementary Material for this paper is available online at https://dx.doi.org/10.2166/wst.2020.134.

REFERENCES

Al-Mamun, A., Ahmad, W., Baawain, M. S., Khadem, M. & Dhar, B. R. 2018 A review of microbial desalination cell technology: configurations, optimization and applications. *J. Cleaner Prod.* **183**, 458–480.

APHA 2012 *Standard Methods for Examination of Water And Wastewater*, 22nd edn. American Public Health Association/American Water Works Association/Water Environment Federation, Washington DC, USA.

Arana, T. J. & Gude, V. G. 2018 A microbial desalination process with microalgae biocathode using sodium bicarbonate as an inorganic carbon source. *Int. Biodeterior. Biodegrad.* **130**, 91–97.

Ashwaniy, V. R. V. & Perumalsamy, M. 2017 Reduction of organic compounds in petro-chemical industry effluent and desalination using *Scenedesmus abundans* algal microbial desalination cell. *J. Environ. Chem. Eng.* **5**, 5961–5967.

Babauta, J., Renslow, R., Lewandowski, Z. & Beyenal, H. 2012 Electrochemically active biofilms: facts and fiction. A review. *Biofouling* **28**, 789–812.

Baranitharan, E., Khan, M. R., Prasad, D. M. R., Teo, W. F. A., Tan, G. Y. A. & Jose, R. 2015 Effect of biofilm formation on the performance of microbial fuel cell for the treatment of palm oil mill effluent. *Bioprocess Biosyst. Eng.* **38**, 15–24.

Bond, D. R. & Lovley, D. R. 2003 Electricity production by *Geobacter sulfurreducens* attached to electrodes. *Appl. Environ. Microbiol.* **69**, 1548–1555.

Cao, X., Huang, X., Liang, P., Xiao, K., Zhou, Y., Zhang, X. & Logan, B. E. 2009 A new method for water desalination using microbial desalination cells. *Environ. Sci. Technol.* **43**, 7148–7152.

Cao, X., Wang, H., Zhang, S., Nishimura, O. & Li, X. 2018 Azo dye degradation pathway and bacterial community structure in biofilm electrode reactors. *Chemosphere* **208**, 219–225.

Caranto, J. D., Vilbert, A. C. & Lancaster, K. M. 2016 *Nitrosomonas europaea* cytochrome p460 is a direct link between nitrification and nitrous oxide emission. *Proc. Natl. Acad. Sci. USA* **113**, 14704–14709.

Cecconet, D., Molognoni, D., Callegari, A. & Capodaglio, A. G. 2018 Agro-food industry wastewater treatment with microbial fuel cells: energetic recovery issues. *Int. J. Hydrogen Energy* **43**, 500–511.

Cecconet, D., Bolognesi, S., Callegari, A. & Capodaglio, A. G. 2019 Controlled sequential biocathodic denitrification for contaminated groundwater bioremediation. *Sci. Total Environ.* **651**, 3107–3116.

Chen, D., Yang, K. & Wang, H. 2016 Effects of important factors on hydrogen-based autotrophic denitrification in a bioreactor. *Desalin. Water Treat.* **57**, 3482–3488.

Cheng, H.-Y., Liang, B., Mu, Y., Cui, M.-H., Li, K., Wu, W.-M. & Wang, A.-J. 2015 Stimulation of oxygen to bioanode for energy recovery from recalcitrant organic matter aniline in microbial fuel cells (MFCs). *Water Res.* **81**, 72–83.

Cheng, H.-Y., Tian, X.-D., Li, C.-H., Wang, S.-S., Su, S.-G., Wang, H.-C., Zhang, B., Sharif, H. M. A. & Wang, A.-J. 2017 Microbial photoelectrotrophic denitrification as a sustainable and efficient way for reducing nitrate to nitrogen. *Environ. Sci. Technol.* **51**, 12948–12955.

Christoff, A., Sereia, A., Boberg, D., Moraes, R. & Oliveira, L. 2017 *Bacterial Identification through Accurate Library Preparation and High-Throughput Sequencing*. Neoprospecta Microbiome Technologies, Florianópolis, Brazil.

Clauwaert, P., Rabaey, K., Aelterman, P., De Schamphelaire, L., Pham, T. H., Boeckx, P., Boon, N. & Verstraete, W. 2007 Biological denitrification in microbial fuel cells. *Environ. Sci. Technol.* **41**, 3354–3360.

Desloover, J., Puig, S., Virdis, B., Clauwaert, P., Boeckx, P., Verstraete, W. & Boon, N. 2011 Biocathodic nitrous oxide

removal in bioelectrochemical systems. *Environ. Sci. Technol.* **45**, 10557–10566.

Dong, Y., Liu, J., Sui, M., Qu, Y., Ambuchi, J. J., Wang, H. & Feng, Y. 2017 A combined microbial desalination cell and electrodialysis system for copper-containing wastewater treatment and high-salinity-water desalination. *J. Hazard. Mater.* **321**, 307–315.

Gacitúa, M. A., Muñoz, E. & González, B. 2018 Bioelectrochemical sulphate reduction on batch reactors: effect of inoculum-type and applied potential on sulphate consumption and pH. *Bioelectrochemistry* **119**, 26–32.

Girme, G. 2014 *Algae Powered Microbial Desalination Cells*. Ohio State University, Columbus, OH, USA.

Gude, V. G., Kokabian, B. & Gadhamshetty, V. 2013 Beneficial bioelectrochemical systems for energy, water, and biomass production. *J. Microbiol. Biochem. Technol.* **S6**, 1–14.

Hou, B., Sun, J. & Hu, Y. 2011 Effect of enrichment procedures on performance and microbial diversity of microbial fuel cell for Congo red decolorization and electricity generation. *Appl. Microbiol. Biotechnol.* **90**, 1563–1572.

Hui, W. J., David, E.-M. & Huang, J. (in press) Using *C. vulgaris* assisted microbial desalination cell as a green technology in landfill leachate pre-treatment: a factor-performance relation study. *J. Water Reuse Desalin.*

Ishii, S., Shimoyama, T., Hotta, Y. & Watanabe, K. 2008 Characterization of a filamentous biofilm community established in a cellulose-fed microbial fuel cell. *BMC Microbiol.* **8**, 6.

Jothinathan, D. & Wilson, R. T. 2018 Performance of *Paracoccus homiensis* DRR-3 in microbial fuel cell with membranes. *Int. J. Ambient Energy* **39**, 573–580.

Katuri, K. P., Scott, K., Head, I. M., Picioreanu, C. & Curtis, T. P. 2011 Microbial fuel cells meet with external resistance. *Bioresour. Technol.* **102**, 2758–2766.

Kim, Y. & Logan, B. E. 2011 Series assembly of microbial desalination cells containing stacked electrodialysis cells for partial or complete seawater desalination. *Environ. Sci. Technol.* **45**, 5840–5845.

Kizilet, A., Akman, D., Akgul, V., Cirik, K. & Cinar, O. 2015 Biocathode application in microbial fuel cells: organic matter removal and denitrification. In: *2015 IEEE 15th International Conference on Environment and Electrical Engineering (EEEIC)*. IEEE, pp. 677–682.

Kokabian, B. & Gude, V. G. 2013 Photosynthetic microbial desalination cells (PMDCs) for clean energy, water and biomass production. *Environ. Sci. Processes Impacts* **15**, 2178–2185.

Kokabian, B., Ghimire, U. & Gude, V. G. 2018a Water deionization with renewable energy production in microalgae – microbial desalination process. *Renew. Energy* **122**, 354–361.

Kokabian, B., Gude, V. G., Smith, R. & Brooks, J. P. 2018b Evaluation of anammox biocathode in microbial desalination coupled with wastewater treatment. *Chem. Eng. J.* **342**, 410–419.

Lefebvre, O., Al-Mamun, A. & Ng, H. Y. 2008 A microbial fuel cell equipped with a biocathode for organic removal and denitrification. *Water Sci. Technol.* **54**, 881–885.

Lewis, K. 1966 Symposium on bioelectrochemistry of microorganisms, IV. Biochemical fuel cells. *Bacteriol. Rev.* **30**, 101–113.

Li, X., Liu, X., Wu, S., Rasool, A., Zuo, J., Li, C. & Liu, G. 2014 Microbial diversity and community distribution in different functional zones of continuous aerobic–anaerobic coupled process for sludge in situ reduction. *Chem. Eng. J.* **257**, 74–81.

Liu, R., Tursun, H., Hou, X., Odey, F., Li, Y., Wang, X. & Xie, T. 2017 Microbial community dynamics in a pilot-scale MFC-AA/O system treating domestic sewage. *Bioresour. Technol.* **241**, 439–447.

Logan, B. E. 2008 *Microbial Fuel Cells*. John Wiley & Sons, Inc., Hoboken, NJ, USA.

Logan, B. E. 2009 Exoelectrogenic bacteria that power microbial fuel cells. *Nat. Rev. Microbiol.* **7**, 375–381.

Logan, B. E., Hamelers, B., Rozendal, R., Schröder, U., Keller, J., Freguia, S., Aelterman, P., Verstraete, W. & Rabaey, K. 2006 Microbial fuel cells: methodology and technology. *Environ. Sci. Technol.* **40**, 5181–5192.

Lovley, D. R. & Nevin, K. P. 2011 A shift in the current: new applications and concepts for microbe-electrode electron exchange. *Curr. Opin. Biotechnol.* **22**, 441–448.

Lovley, D. R. & Phillips, E. J. 1988 Novel mode of microbial energy metabolism: organic carbon oxidation coupled to dissimilatory reduction of iron or manganese. *Appl. Environ. Microbiol.* **54**, 1472–1480.

Meng, F., Jiang, J., Zhao, Q., Wang, K., Zhang, G., Fan, Q., Wei, L., Ding, J. & Zheng, Z. 2014 Bioelectrochemical desalination and electricity generation in microbial desalination cell with dewatered sludge as fuel. *Bioresour. Technol.* **157**, 120–126.

Meng, F., Zhao, Q., Na, X., Zheng, Z., Jiang, J., Wei, L. & Zhang, J. 2017 Bioelectricity generation and dewatered sludge degradation in microbial capacitive desalination cell. *Environ. Sci. Pollut. Res.* **24**, 5159–5167.

Menon, B. B., Dou, Z., Heinhorst, S., Shively, J. M. & Cannon, G. C. 2008 *Halothiobacillus neapolitanus* carboxysomes sequester heterologous and chimeric RubisCO species. *PLoS One* **3**, e3570.

Mologni, D., Puig, S., Balaguer, M. D., Liberale, A., Capodaglio, A. G., Callegari, A. & Colprim, J. 2014 Reducing start-up time and minimizing energy losses of microbial fuel cells using maximum power point tracking strategy. *J. Power Sources* **269**, 403–411.

Mologni, D., Chiarolla, S., Cecconet, D., Callegari, A. & Capodaglio, A. G. 2018 Industrial wastewater treatment with a bioelectrochemical process: assessment of depuration efficiency and energy production. *Water Sci. Technol.* **77**, 134–144.

Perazzoli, S., Bastos, R. B., Santana, F. B. & Soares, H. M. 2018 Biological fuel cells produce bioelectricity with in situ brackish water purification. *Water Sci. Technol.* **78**, 301–309.

Qiao, Y.-J., Qiao, Y., Zou, L., Wu, X.-S. & Liu, J.-H. 2017 Biofilm promoted current generation of *Pseudomonas aeruginosa* microbial fuel cell via improving the interfacial redox reaction of phenazines. *Bioelectrochemistry* **117**, 34–39.

Rotaru, A.-E., Shrestha, P. M., Liu, F., Markovaite, B., Chen, S., Nevin, K. P. & Lovley, D. R. 2014 Direct interspecies electron

transfer between *Geobacter metallireducens* and *Methanosarcina barkeri*. *Appl. Environ. Microbiol.* **80**, 4599–4605.

Saba, B., Christy, A. D., Yu, Z., Co, A. C. & Park, T. 2017 Simultaneous power generation and desalination of microbial desalination cells using *Nannochloropsis salina* (marine algae) versus potassium ferricyanide as catholytes. *Environ. Eng. Sci.* **34**, 185–196.

Santoro, C., Arbizzani, C., Erable, B. & Ieropoulos, I. 2017 Microbial fuel cells: from fundamentals to applications. A review. *J. Power Sources* **356**, 225–244.

Saratale, G. D., Saratale, R. G., Shahid, M. K., Zhen, G., Kumar, G., Shin, H.-S., Choi, Y.-G. & Kim, S.-H. 2017 A comprehensive overview on electro-active biofilms, role of exoelectrogens and their microbial niches in microbial fuel cells (MFCs). *Chemosphere* **178**, 534–547.

Savitzky, A. & Golay, M. 1964 Smoothing and differentiation of data by simplified least-squares procedures. *Anal. Chem.* **3**, 1627–1639.

Schmidt, I., Van Spanning, R. J. M. & Jetten, M. S. M. 2004 Denitrification and ammonia oxidation by *Nitrosomonas europaea* wild-type, and NirK- and NorB-deficient mutants. *Microbiology* **150**, 4107–4114.

Srinivasan, V., Weinrich, J. & Butler, C. 2016 Nitrite accumulation in a denitrifying biocathode microbial fuel cell. *Environ. Sci. Water Res. Technol.* **2**, 344–352.

Sun, Y., De Vos, P. & Willems, A. 2017 Nitrogen assimilation in denitrifier *Bacillus azotoformans* LMG 9581T. *Antonie Van Leeuwenhoek* **110**, 1613–1626.

Tang, R., Wu, D., Chen, W., Feng, C. & Wei, C. 2017 Biocathode denitrification of coke wastewater effluent from an industrial aeration tank: effect of long-term adaptation. *Biochem. Eng. J.* **125**, 151–160.

Vilajeliu-Pons, A., Bañeras, L., Puig, S., Molognoni, D., Vilà-Rovira, A., Hernández-del Amo, E., Balaguer, M. D. & Colprim, J. 2016 External resistances applied to MFC affect core microbiome and swine manure treatment efficiencies. *PLoS One* **11**, e0164044.

Wang, H. & Ren, Z. J. 2013 A comprehensive review of microbial electrochemical systems as a platform technology. *Biotechnol. Adv.* **31**, 1796–1807.

Wang, J., Song, X., Wang, Y., Abayneh, B., Li, Y., Yan, D. & Bai, J. 2016 Nitrate removal and bioenergy production in constructed wetland coupled with microbial fuel cell: establishment of electrochemically active bacteria community on anode. *Bioresour. Technol.* **221**, 358–365.

Wang, J., He, M.-F., Zhang, D., Ren, Z., Song, T. & Xie, J. 2017 Simultaneous degradation of tetracycline by a microbial fuel cell and its toxicity evaluation by zebrafish. *RSC Adv.* **7**, 44226–44233.

Watson, V. J. & Logan, B. E. 2011 Analysis of polarization methods for elimination of power overshoot in microbial fuel cells. *Electrochem. Commun.* **13**, 54–56.

Wen, Q., Zhang, H., Chen, Z., Li, Y., Nan, J. & Feng, Y. 2012 Using bacterial catalyst in the cathode of microbial desalination cell to improve wastewater treatment and desalination. *Bioresour. Technol.* **125**, 108–113.

Wenzel, J., Fuentes, L., Cabezas, A. & Etchebehere, C. 2017 Microbial fuel cell coupled to biohydrogen reactor: a feasible technology to increase energy yield from cheese whey. *Bioprocess Biosyst. Eng.* **40**, 807–819.

Xing, W., Li, J.-L., Li, D., Hu, J., Deng, S.-H., Cui, Y. & Yao, H. 2018 Stable-isotope probing reveals activity and function of autotrophic and heterotrophic denitrifiers in nitrate removal from organic-limited wastewater. *Environ. Sci. Technol.* **52**, 7867–7875.

Xu, D., Xiao, E., Xu, P., Zhou, Y., He, F., Zhou, Q., Xu, D. & Wu, Z. 2017 Performance and microbial communities of completely autotrophic denitrification in a bioelectrochemically-assisted constructed wetland system for nitrate removal. *Bioresour. Technol.* **228**, 39–46.

Yoganathan, K. & Ganesh, P. 2015 Electrogenicity assessment of *Bacillus subtilis* and *Bacillus megaterium* using microbial fuel cell technology. *Int. J. Appl. Res.* **1**, 435–438.

Young, B., Lae-Jung, I. & Hyun-Park, D. 2011 Enrichment of CO_2 -fixing bacteria in cylinder-type electrochemical bioreactor with built-in anode compartment. *J. Microbiol. Biotechnol.* **21**, 590–598.

Zhang, G., Jiao, Y. & Lee, D.-J. 2015 A lab-scale anoxic/oxic-bioelectrochemical reactor for leachate treatments. *Bioresour. Technol.* **186**, 97–105.

Zhang, G., Jiao, Y. & Lee, D.-J. 2016 Leachate treatment using anoxic/oxic-bioelectrochemical reactor with intermittent aeration. *J. Taiwan Inst. Chem. Eng.* **58**, 401–406.

Zhang, E., Wang, F., Yu, Q., Scott, K., Wang, X. & Diao, G. 2017 Durability and regeneration of activated carbon air-cathodes in long-term operated microbial fuel cells. *J. Power Sources* **360**, 21–27.

Zhang, L., Fu, G. & Zhang, Z. 2019 High-efficiency salt, sulfate and nitrogen removal and microbial community in biocathode microbial desalination cell for mustard tuber wastewater treatment. *Bioresour. Technol.* **289**, 121630.

Zuo, K., Chen, M., Liu, F., Xiao, K., Zuo, J., Cao, X., Zhang, X., Liang, P. & Huang, X. 2018 Coupling microfiltration membrane with biocathode microbial desalination cell enhances advanced purification and long-term stability for treatment of domestic wastewater. *J. Membr. Sci.* **547**, 34–42.

First received 28 November 2019; accepted in revised form 18 March 2020. Available online 25 March 2020